

GDO: Gradual Domain Osmosis

Zixi Wang^{*1,2} Yubo Huang^{*1}

Abstract

In this paper, we propose a new method called Gradual Domain Osmosis, which aims to solve the problem of smooth knowledge migration from source domain to target domain in Gradual Domain Adaptation (GDA). Traditional Gradual Domain Adaptation methods mitigate domain bias by introducing intermediate domains and self-training strategies, but often face the challenges of inefficient knowledge migration or missing data in intermediate domains. In this paper, we design an optimisation framework based on the hyperparameter λ by dynamically balancing the loss weights of the source and target domains, which enables the model to progressively adjust the strength of knowledge migration (λ incrementing from 0 to 1) during the training process, thus achieving cross-domain generalisation more efficiently. Specifically, the method incorporates self-training to generate pseudo-labels and iteratively updates the model by minimising a weighted loss function to ensure stability and robustness during progressive adaptation in the intermediate domain. The experimental part validates the effectiveness of the method on rotated MNIST, colour-shifted MNIST, portrait dataset and forest cover type dataset, and the results show that it outperforms existing baseline methods. The paper further analyses the impact of the dynamic tuning strategy of the hyperparameter λ on the performance through ablation experiments, confirming the advantages of progressive domain penetration in mitigating the domain bias and enhancing the model generalisation capability. The study provides a theoretical support and practical framework for asymptotic domain adaptation and expands its application potential in dynamic environments.

^{*}Equal contribution ¹University of Electronic Science and Technology of China, Sichuan, China ²Southwest Jiaotong University, Sichuan, China. Correspondence to: Zixi Wang <zixi-wang@outlook.com>, Yubo Huang <ybforever@my.swjtu.edu.cn>.

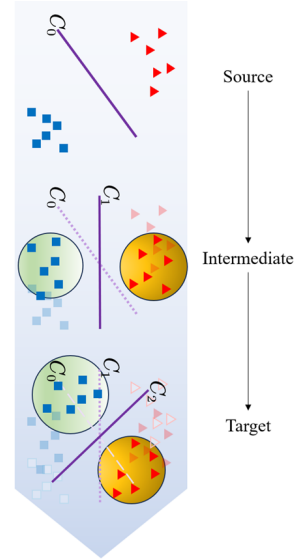


Figure 1. An example of domain shift. The red is source domain and the blue is target domain. The yellow regions are assumed to have zero support in the target distribution.

1. Introduction

One of the core challenges in machine learning is the domain shift, which occurs when the distribution of data in the training domain (source domain) differs significantly from the distribution in the target domain (Ovadia et al., 2019; Pan & Yang, 2009), as shown in Figure 1. This problem is prevalent in real-world applications where labeled data in the target domain is scarce or expensive to obtain. Domain adaptation (DA) (Li et al., 2016; Zhao et al., 2020) has become an essential strategy for transferring knowledge across domains, particularly in situations where data distributions between the source and target domains are misaligned. Unsupervised domain adaptation (UDA) aims to address this issue by utilizing unlabeled data from the target domain to enhance model performance (Liu et al., 2022). However, UDA struggles when domain shifts are large, or when intermediate domain data is minimal or nonexistent.

To address these limitations, recent advances have introduced Gradual Domain Adaptation (GDA), a framework that aims to reduce the drastic shift between domains by employing a more controlled and stepwise knowledge trans-

fer process. (Farshchian et al., 2018; Kumar et al., 2020). (Kumar et al., 2020) explored this gradual approach and proposed strategies to improve model stability during adaptation, demonstrating that such a progressive transfer process can significantly mitigate the adverse effects of domain shifts, but challenges remain in efficiently transitioning between domains and maintaining model performance. (Chen & Chao, 2021) further refined the GDA framework by introducing new techniques for generating intermediate domains and enhancing the smoothness of the adaptation process. Their approach shows promising results in various tasks, including image classification and object detection, where large domain shifts are prevalent. However, the migration of knowledge across intermediate domains is still suboptimal, leading to slower convergence times and potential overfitting issues (He et al., 2023). In addition, (Marsden et al., 2024) examined the risks of instability when adapting models through numerous intermediate domains, highlighting the need for novel techniques to control the adaptation process more precisely.

In this work, we aim to address the limitations of GDA by focusing on the efficient migration of knowledge between domains, reducing the risk of instability, and exploring novel methods to improve the effectiveness of the gradual adaptation process. First, we propose a new optimization objective that balances source and target losses dynamically. Secondly, we introduce a self-training mechanism that iteratively refines the model using pseudo-labeled data. Our contributions are as follows:

- We designed an optimization framework, namely Gradual Domain Osmosis (GDO), based on the hyperparameter λ to achieve more efficient knowledge transfer by dynamically adjusting the weights of the loss functions in the source and target domains. As the training process progresses, the λ value gradually increases from 0 to 1, allowing the model to gradually adjust the strength of knowledge transfer, thereby more effectively achieving cross-domain generalization.
- In order to ensure stability and robustness during the gradual adaptation process in the intermediate domain, the GDO method combines self-training technology to generate pseudo labels and iteratively updates the model by minimizing the weighted loss function. This method helps to alleviate the performance degradation caused by domain shift and improve the generalization ability of the model between different domains.
- The paper verifies the effectiveness of the proposed method through experiments on Rotated MNIST, color-shifted MNIST, Portrait datasets, and Cover type datasets. The results show that this method outperforms existing baseline methods.

2. Related Work

Domain Generalization Domain Generalization (DG) aims to train models that generalize well to unseen target domains without accessing target data during training (Muandet et al., 2013; Dou et al., 2019). Unlike UDA, DG does not assume any availability of target domain data, making it highly applicable in scenarios where target environments are unknown or continuously evolving. Strategies in DG include learning robust feature representations through data augmentation, meta-learning, and enforcing invariance to domain-specific variations (Bui et al., 2021; Wang et al., 2022b; Li et al., 2018). Recent advancements have focused on leveraging meta-learning frameworks to simulate domain shifts during training, thereby preparing models for unseen domains (Wang et al., 2022a).

Unsupervised Domain Adaptation Unsupervised Domain Adaptation (UDA) tackles the challenge of domain shifts—discrepancies between source (training) and target (testing) domains—by leveraging only unlabeled data from the target domain (Farahani et al., 2021; Ganin & Lempitsky, 2015b; Tzeng et al., 2017). The goal is to learn robust, domain-invariant features that enable a model to generalize despite distribution mismatches (Pan & Yang, 2009; Hoffman et al., 2018). Common approaches include aligning source and target feature distributions via measures like maximum mean discrepancy (Chen et al., 2020; Yan et al., 2017) or through adversarial learning frameworks (Zhang et al., 2018; Volpi et al., 2018). However, recent studies (Kang et al., 2019; Tang & Jia, 2020; Yang et al., 2020; Zhao et al., 2019; Kumar et al., 2020) reveal that naive alignment can introduce misalignment and fail when the shift is severe or the target data present novel variations outside the source’s coverage.

Gradual Domain Adaptation Gradual Domain Adaptation (GDA) addresses scenarios where data shift gradually rather than abruptly, allowing the overall shift to be decomposed into a sequence of smaller steps (Farshchian et al., 2018; Kumar et al., 2020). By introducing intermediate domains and employing self-training (Xie et al., 2020), GDA bridges large source–target gaps more effectively and has sparked both theoretical (Wang et al., 2022a) and algorithmic (Chen & Chao, 2021; Abnar et al., 2021) advancements. Key strategies involve generating intermediate distributions via gradient flow-based geodesic paths (Zhuang et al., 2024), style-transfer interpolation (Marsden et al., 2024), and optimal transport (He et al., 2023), while complementary methods leverage normalizing flows (Sagawa & Hino, 2022), source–target data ratio adjustments (Zhang et al., 2021), domain sequence discovery (Chen & Chao, 2021), and adversarial self-training (Shi & Liu, 2024) to enhance robustness and generalization.

3. Problem Setup

Domain Space Let $\mathcal{Z} = \mathcal{X} \times \mathcal{Y}$ be the measurable instance space, in which $\mathcal{X} \subseteq \mathbb{R}^d$ is the input space in d -dimensional space and $\mathcal{Y} = \{1, 2, \dots, k\}$ is the label space, where k is the number of classes.

Gradually shifting Domain In the gradually domain setting (Kumar et al., 2020), we have $n+1$ domains indexed by $0, 1, \dots, n$, where the domain 0 is the source domain, domain n is the target domain and the intermediate domains are indexed by $1, 2, \dots, n-1$. Those domains distribute over the instance space \mathcal{Z} , denoted as $\mathcal{D}_0, \mathcal{D}_1, \dots, \mathcal{D}_n$.

Classification and Loss The goal of classification is to learn a model $C : \mathcal{X} \rightarrow \mathcal{Y}$ that maps input features x from the training data set $\mathcal{D} = \{(x, y)\}$ to their corresponding labels y . Considering the loss function l , the classifier benefit on \mathcal{D}_t is denoted by C , defined as:

$$C = \arg \min_C \mathbb{E}_{(x,y) \sim \mathcal{D}_t} [l(C(x), y)]. \quad (1)$$

Domain Adaptation In domain adaptation settings, there are two different domains involved: the source domain \mathcal{D}_S and the target domain \mathcal{D}_T . The model is trained on data from the source domain but is expected to generalize to the target domain, where the distribution of data may be different. The goal is to improve the model’s performance on the target domain despite the lack of labeled data in the target domain, using the knowledge learned from the source domain.

Gradual Domain Adaptation The goal of gradual domain adaptation is to learn a classifier C that generalizes well to the target domain \mathcal{D}_n by progressively transferring knowledge from the labeled source domain \mathcal{D}_0 and a series of unlabeled intermediate domains $\mathcal{D}_1, \mathcal{D}_2, \dots, \mathcal{D}_{n-1}$. The adaptation process involves multi-step pseudo-labeling and self-training, where the model C_0 is trained on the source domain and then adapted to the intermediate domains by the following self-training procedure $\text{ST}(C_t, \mathcal{D}_t)$:

$$\text{ST}(C_t, \mathcal{D}_t) = \arg \min_{C'} \mathbb{E}_{x \sim \mathcal{D}_t} [l(C'(x), \hat{y}_t(x))]. \quad (2)$$

In particular, $\hat{y}_t(x) = \text{sign}(C_t(x))$ is the pseudo-label generated by the model C_t for unlabeled data of \mathcal{D}_t , where \mathcal{D}_t denotes the unlabeled intermediate domain. Meanwhile, C' is the next learned model, also denoted by C_{t+1} .

4. Methodology

This work proposes Gradual Domain Osmosis (GDO), which reconstructs traditional self-training paradigms through a triple adaptive mechanism. The framework of

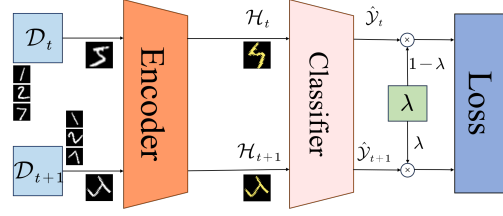


Figure 2. The framework of our GDO. It is designed to adapt a model from a source domain to a target domain in a smooth and controlled manner. The hyperparameter λ controls the trade-off between the two domains: when $\lambda = 0$, the model focuses entirely on the source domain, and as λ increases to 1, the model progressively shifts its focus to the target domain. Pseudo-labels, generated by the model itself, guide the learning process, ensuring gradual and stable adaptation.

GDO is shown in Figure 2 Consider the following optimization problem:

$$\min_C (1 - \lambda) \mathbb{E}_{x \sim \mathcal{D}_i} [l(C(x), \text{sign}(C(x)))] + \lambda \mathbb{E}_{x \sim \mathcal{D}_{i+1}} [l(C(x), \text{sign}(C(x)))] \quad (3)$$

Here λ is a hyperparameter that balances the trade-off between the source and target domains. With an increasing λ from 0 to 1, the knowledge gradually transfers from the source domain to the target domain. For a domain sequence $\{\mathcal{D}_t\}_{t=0}^n$, where each domain contains m data batches $\{B_{t,1}, \dots, B_{t,m}\}$, we define a time-varying classifier $C^{(t,k)}$ representing the model after the k -th batch update in domain t . Its evolution follows:

$$C^{(t,k+1)} = \Phi \left(C^{(t,k)}, B_{t,k}, B_{t,k+1} \right) \quad (4)$$

where Φ is an incremental optimization operator based on the following objective:

$$\begin{aligned} \Phi = \arg \min_{C'} \mathbb{E}_{x \sim B_{t,k}} \left[\underbrace{\ell_{\text{ce}}(C'(x), \hat{y}^{(t,k)}(x))}_{\text{Pseudo-Label Consistency}} \right] \\ + \alpha \underbrace{\mathbb{E}_{x \sim B_{t,k+1}} [\ell_{\text{margin}}(C'(x))]}_{\text{Prospective Margin Maximization}} \\ + \beta \underbrace{D_{\text{KL}}(p(C') \| p(C^{(t,k)}))}_{\text{Knowledge Distillation Constraint}} \end{aligned} \quad (5)$$

where dynamically generated hard pseudo-labels are represented as $\hat{y}^{(t,k)}(x) = \arg \max_y C^{(t,k)}(x)_y$, indicating the most likely class label for sample x at stage t and batch k according to the current classifier $C^{(t,k)}$. The margin loss is defined as $\ell_{\text{margin}}(z) = \max(0, 1 - (\max_j z_j - \max_{j \neq \hat{y}} z_j))$, where z represents the unnormalized scores (logits) output by the model.

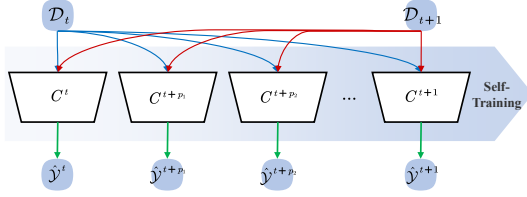


Figure 3. The process of Gradual Domain Adaptation with Dynamic Pseudo-Labeling and Self-Training. The diagram demonstrates the generation of hard pseudo-labels at each stage of the domain adaptation process. The classifiers $C^{(t,k)}$ are progressively updated, using a dual-timescale update rule for intra-domain and inter-domain adaptation. The model updates the feature extractor parameters θ in a high-frequency manner and classifier head parameters ϕ in a low-frequency manner to facilitate smooth domain transitions. This approach promotes rapid domain adaptation and minimizes the loss between predictions and pseudo-labels across the domains \mathcal{D}_t and \mathcal{D}_{t+1} .

To achieve cross-batch and cross-domain adaptation, we design a dual-timescale update rule:

$$\begin{cases} \theta^{(t,k+1)} = \theta^{(t,k)} - \eta_t \nabla_{\theta} \mathcal{L}_{\text{intra}}(\theta^{(t,k)}, B_{t,k}) \\ \phi^{(t+1,0)} = \phi^{(t,m)} - \zeta \nabla_{\phi} \mathcal{L}_{\text{inter}}(\phi^{(t,m)}, \mathcal{D}_t, \mathcal{D}_{t+1}) \end{cases} \quad (6)$$

where θ is the feature extractor parameters updated via high-frequency batch-wise adaptation. ϕ is classifier head parameters updated via low-frequency domain transition. $\mathcal{L}_{\text{intra}} = \ell_{\text{ce}} + \alpha \ell_{\text{margin}}$ drives rapid intra-domain adaptation. $\mathcal{L}_{\text{inter}} = \mathbb{E}_{x \sim \mathcal{D}_t \cup \mathcal{D}_{t+1}} [\|\nabla_x C(x)\|_2^2]$ is the gradient alignment loss for smooth domain transitions.

As shown in Fig. 3, the gradual classifier C is learned by minimizing the objective function above. The pseudo-labels are generated by the model itself, and the model is updated by minimizing the loss between the model’s prediction and the pseudo-labels. C can be progressively updated by the following equation:

$$\begin{aligned} C^{(i+\lambda)} &= \text{ST}(C, \lambda, \mathcal{D}_i, \mathcal{D}_{i+1}) = \arg \min_{C'} \\ &(1 - \lambda) \mathbb{E}_{x \sim \mathcal{D}_i} [l(C'(x), \text{sign}(C(x)))] \\ &+ \lambda \mathbb{E}_{x \sim \mathcal{D}_{i+1}} [l(C'(x), \text{sign}(C(x)))] \end{aligned} \quad (7)$$

Therefore, The dual-timescale optimization framework is implemented as algorithm 1:

Algorithm 1 Gradual Domain Osmosis (GDO)

input Source batches $\{B_{0,k}\}_{k=1}^m$, domain sequence $\{\mathcal{D}_t\}_{t=1}^n$, initial model $C^{(0,0)}$
output Adapted model $C^{(n,m)}$

- 1: **for** $t = 0$ TO $n - 1$ **do**
- 2: **for** $k = 0$ TO $m - 1$ **do**
- 3: Fetch batch $B_{t,k}$, generate pseudo-labels: $\hat{y}^{(t,k)} = \arg \max_y C^{(t,k)}(x)_y$
- 4: Compute intra-domain loss: $\mathcal{L}_{\text{intra}} = \ell_{\text{ce}} + \alpha \ell_{\text{margin}}$
- 5: Update feature extractor: $\theta^{(t,k+1)} \leftarrow \theta^{(t,k)} - \eta_t \nabla_{\theta} \mathcal{L}_{\text{intra}}$
- 6: Warm-up next batch: Compute gradient alignment $\mathcal{L}_{\text{inter}}$ for $B_{t,k+1}$
- 7: **end for**
- 8: Inter-domain transfer: $\phi^{(t+1,0)} \leftarrow \phi^{(t,m)} - \zeta \nabla_{\phi} \mathbb{E}[\mathcal{L}_{\text{inter}}]$
- 9: **end for**

5. Theoretical Arguments

5.1. Error Propagation Dynamics

Let \mathcal{H} be the hypothesis class with VC-dimension $d_{\mathcal{H}}$. For any batch B_t, k , we define the empirical risk $\hat{R}_t^{(k)}(C)$ as follows:

$$\hat{R}_t^{(k)}(C) = \frac{1}{|B_{t,k}|} \sum_{x \in B_{t,k}} \ell(C(x), \hat{y}^{(t,k)}(x)) \quad (8)$$

where $\hat{y}^{(t,k)}(x)$ represents the pseudo-label for the input x , and ℓ is the loss function. The population risk $R_t(C)$ is defined as the expected loss over the distribution \mathcal{D}_t :

$$R_t(C) = \mathbb{E}_{x \sim \mathcal{D}_t} [\ell(C(x), y(x))] \quad (9)$$

Lemma 1 (Pseudo-Label Consistency) We want to bound the difference between the empirical risk $\hat{R}_t^{(k)}(C)$ and the population risk $R_t(C)$. For $\rho(B_{t,k}, B_{t,k+1}) \leq \epsilon$, the pseudo-label discrepancy satisfies:

$$|\hat{R}_t^{(k)}(C) - R_t(C)| \leq \sqrt{\frac{2d_{\mathcal{H}} \log(2em/d_{\mathcal{H}})}{m}} + \epsilon L_{\ell} R \quad (10)$$

Proof We apply Rademacher complexity bounds with distribution shift:

$$\mathbb{E}[\sup_{C \in \mathcal{H}} |\hat{R}_t^{(k)}(C) - R_t(C)|] \leq 2\mathfrak{R}_m(\mathcal{H}) + L_{\ell} W_1(B_{t,k}, \mathcal{D}_t) \quad (11)$$

Here, $\mathfrak{R}_m(\mathcal{H})$ is the Rademacher complexity of the hypothesis class \mathcal{H} , and $W_1(B_{t,k}, \mathcal{D}_t)$ is the Wasserstein distance between the empirical distribution over the batch $B_{t,k}$ and the true data distribution \mathcal{D}_t . Using the fact that $W_1(B_{t,k}, \mathcal{D}_t) \leq \epsilon R$ and the bound for $\mathfrak{R}_m(\mathcal{H})$, we get the desired result:

$$|\hat{R}_t^{(k)}(C) - R_t(C)| \leq \sqrt{\frac{2d_{\mathcal{H}} \log(2em/d_{\mathcal{H}})}{m}} + \epsilon L_{\ell} R \quad (12)$$

5.2. Lyapunov Stability Analysis

Next, we define the Lyapunov function $V(t, k)$, which incorporates both the error and the parameter drift:

$$V(t, k) = \text{Err}_{t,k} + \lambda \|\theta^{(t,k)} - \theta^{(t,k-1)}\|^2 \quad (13)$$

where $\text{Err}_{t,k} = \mathbb{E}_{x \sim \mathcal{D}_t} [\mathbb{I}(C^{(t,k)}(x) \neq y(x))]$ is the error at time t and iteration k , and λ is a constant.

Lemma 2 (Lyapunov Drift) Under gradient-based updates, the Lyapunov function satisfies:

$$V(t, k+1) \leq (1 - \eta_t \mu) V(t, k) + \eta_t^2 \sigma^2 + c\epsilon \sqrt{\frac{\log m}{m}} \quad (14)$$

where μ is the strong convexity parameter, σ^2 bounds the gradient variance, $c\epsilon \sqrt{\frac{\log m}{m}}$ accounts for the discrepancy between batches.

Proof Sketch To compute the drift $\Delta V = V(t, k+1) - V(t, k)$, we break it into two terms: the optimization term and the parameter drift term.

Optimization Term: $\text{Err}_{t,k+1} - \text{Err}_{t,k}$

By applying SGD convergence analysis, we get:

$$\text{Err}_{t,k+1} \leq \text{Err}_{t,k} - \eta_t \mu \|\nabla \text{Err}_{t,k}\|^2 + \eta_t^2 \sigma^2 \quad (15)$$

Parameter Drift Term: $\|\theta^{(t,k+1)} - \theta^{(t,k)}\|^2$

Using the update rule $\theta^{(t,k+1)} = \theta^{(t,k)} - \eta_t g_t$, we get:

$$\|\theta^{(t,k+1)} - \theta^{(t,k)}\|^2 = \eta_t^2 \|g_t\|^2 \leq \eta_t^2 G^2 \quad (16)$$

Combining these terms, we get the Lyapunov drift bound:

$$V(t, k+1) \leq (1 - \eta_t \mu) V(t, k) + \eta_t^2 \sigma^2 + c\epsilon \sqrt{\frac{\log m}{m}} \quad (17)$$

To bound the total error over T domains, we telescope the Lyapunov inequality over the T domains and m batches:

$$V(T, 0) \leq V(0, 0) \prod_{t=1}^T (1 - \eta_t \mu) + \sum_{t=1}^T \left(\eta_t^2 \sigma^2 + c\epsilon \sqrt{\frac{\log m}{m}} \right) \quad (18)$$

Substitute the geometric series summation:

$$\prod_{t=1}^T (1 - \eta_t \mu) \leq e^{-\mu \sum_{t=1}^T \eta_t} \leq e^{-\kappa \gamma_0 T} \quad (19)$$

where $\kappa = \frac{\mu}{\gamma_0} 2$ and $\eta_t = \frac{\gamma_0}{1 + \epsilon t}$. The second term accumulates as:

$$\begin{aligned} \sum_{t=1}^T \eta_t^2 \sigma^2 &\leq \sigma^2 \gamma_0^2 \sum_{t=1}^T \frac{1}{(1 + \epsilon t)^2} \\ &\leq \frac{c_1 \epsilon}{\gamma_0} \sqrt{\frac{T}{m}} \end{aligned} \quad (20)$$

The generalization error term follows from Lemma 1:

$$\sum_{t=1}^T c\epsilon \sqrt{\frac{\log m}{m}} \leq c_2 \sqrt{\frac{\log(mT/\delta)}{m}} \quad (21)$$

Combining all components yields the final error bound:

$$\text{Err}_T \leq \text{Err}_0 \cdot e^{-\kappa \gamma_0 T} + \frac{c_1 \epsilon}{\gamma_0} \sqrt{\frac{T}{m}} + c_2 \sqrt{\frac{\log(mT/\delta)}{m}} \quad (22)$$

where $\kappa = \frac{\mu \gamma_0}{2}$ reflects the interaction between optimization rate and initial margin. $c_1 = \frac{\sigma^2 \gamma_0^2}{\sqrt{2}}$ captures the variance-margin tradeoff. $c_2 = 2c\sqrt{\log(1/\delta)}$ depends on distribution shift and confidence level.

6. Experiments

6.1. Environments Setup

To empirically validate our method, we examine gradual self-training on two synthetic and two real datasets, including Rotated MNIST, Color-Shift MNIST, Portraits Dataset (Ginosar et al., 2015) and Cover Type Dataset (Blackard, 1998).

Table 1. Benchmarks Comparison on different datasets, including UDA methods and GDA methods.

UDA/GDA methods	Rotated MNIST	Color-Shift MNIST	Portraits	Cover Type
DANN (Ganin et al., 2016)	44.23	56.5	73.8	-
DeepCoral (Sun & Saenko, 2016)	49.6	63.5	71.9	-
DeepJDOT (Damodaran et al., 2018)	51.6	65.8	72.5	-
GST (Kumar et al., 2020)	83.8	74.0	82.6	73.5
IDOL (Chen & Chao, 2021)	87.5	-	85.5	-
GOAT (He et al., 2023)	86.4	91.8	83.6	69.9
GGF (Zhuang et al., 2024)	67.72	-	86.16	-
CNF (Sagawa & Hino, 2025)	62.55	-	84.57	-
GDO (Ours)	97.6	98.3	86.1	74.2

Rotated MNIST This is a semi-synthetic dataset based on the widely used MNIST dataset (Deng, 2012). Following He et al. (2023), it consists of 50,000 images for the source domain (original MNIST images) and the same 50,000 images rotated by 45 degrees to form the target domain. The intermediate domains are evenly distributed between the source and target domains, with rotations gradually changing from 0 to 45 degrees.

Color-Shift MNIST This dataset is built by applying a color shift to the MNIST dataset. Following He et al. (2023), it consists of the same 50,000 images as the source domain, in which the pixel values are normalized to $[0, 1]$, with the pixel values shifted to be in the range $[1, 2]$ for the target domain. The intermediate domains are evenly distributed between the source and target domains, resulting in various color shifts.

Portraits Dataset (Ginosar et al., 2015) This dataset contains portraits of high school seniors from 1905 to 2013, primarily used for gender classification tasks. Following Kumar et al. (2020), the dataset is arranged chronologically, from front to back, with every 2000 images set as a domain, and a total of 9 domains are set, containing the first being the source domain, the middle seven intermediate domains, and the last being the target domain. All data is processed to 32 x 32 pixel size.

Cover Type Dataset (Blackard, 1998) The Cover Type dataset is a tabular dataset designed to predict the type of forest cover and contains 54 features. Following Kumar et al. (2020), we focus on the first two categories of forest cover: spruce fir and Rocky Mountain pine. We sort the dataset based on the horizontal distance from the nearest water body. The first 50,000 data are used as the source domain, followed by every 40,000 subsequent data, creating a total of ten intermediate domains, and the last 50,000 data are treated as the target domain.

Implementation For the Rotated MNIST, Color-Shift MNIST, and Portraits datasets, a convolutional neural net-

work (CNN) architecture was implemented consisting of three convolutional layers, each with 32 channels. The encoder is followed by a fully connected classifier with two hidden layers, each containing 256 units. For the Cover Type dataset, a similar architecture was employed, utilizing three fully connected layers with ReLU activations, where the sizes of the hidden layers increase progressively from 128 to 256 to 512 units. The final layer corresponds to the number of classes in the dataset. Optimization was performed using the Adam optimizer (Kingma & Ba, 2014), while regularization was achieved via Dropout (Srivastava et al., 2014). Batch Normalization (Ioffe & Szegedy, 2015) was applied to enhance the stability of training. The transport network architecture integrates generators, which are constructed using a residual block containing three linear layers. The discriminator comprises three linear layers, each with 128 hidden units, and employs ReLU activations. The number of intermediate domains generated between the source and target domains was treated as a hyperparameter, with model performance evaluated for 0, 1, 2, 3, or 4 intermediate domains. All experiments were conducted on NVIDIA RTX 4090 GPUs.

Benchmarks To verify the effectiveness of our GDO, we compare it with several state-of-the-art (SOTA) methods, including 3 UDA methods, DANN (Ganin & Lempitsky, 2015a), DeepCoral (Sun & Saenko, 2016), DeepJDOT (Damodaran et al., 2018) and 5 GDA methods, GST (Kumar et al., 2020), IDOL (Chen & Chao, 2021), GOAT (He et al., 2023), GGF (Zhuang et al., 2024), and GNF (Sagawa & Hino, 2025) using the same training datasets with ours.

6.2. Results

Table 1 demonstrates our method’s superior performance across all benchmark datasets compared to existing UDA and GDA approaches. Our GDO achieves state-of-the-art results with significant margins. Specifically, Our GDO achieved 11.2%, 6.5%, 0.94%, and 4.3% improvement in accuracy compared to the second-best results on Rotated MNIST, Color-Shift MNIST, Portraits, and Cover Type

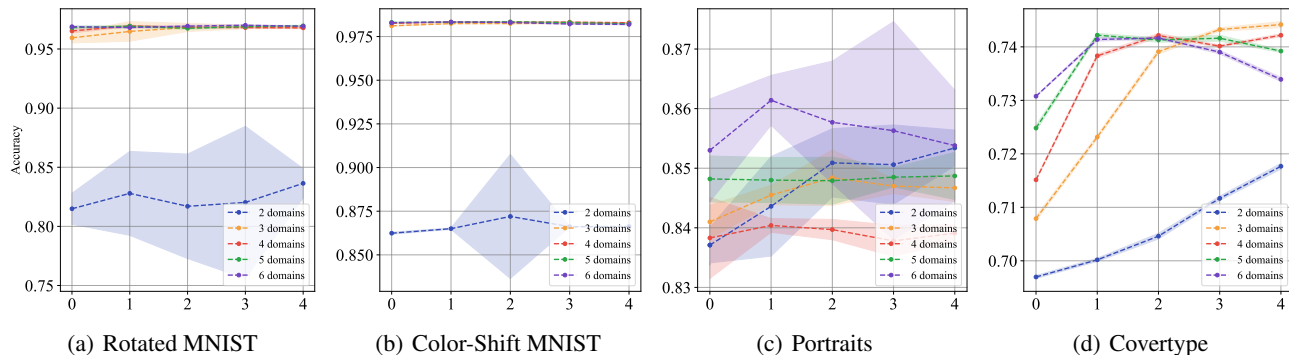


Figure 4. Ablation experiments with different domain conditions are conducted on four datasets. Two domains represent no intermediate domains (only source domain and target domain), and the added domains are all intermediate domains.

Table 2. Comparison of the accuracy of our method for different given intermediate domains (including source and target domains) on the **Rotated MNIST** dataset, as well as the 95% confidence interval of the mean across 5 runs.

# Given Domains	# Inter-domain counts in GDO				
	0	1	2	3	4
2	81.5 ± 1.3	82.8 ± 3.5	81.7 ± 4.4	82.0 ± 6.4	83.6 ± 1.2
3	95.9 ± 0.4	96.5 ± 0.8	96.8 ± 0.3	96.9 ± 0.1	96.8 ± 0.1
4	96.5 ± 0.2	96.9 ± 0.1	96.8 ± 0.0	96.8 ± 0.0	96.8 ± 0.1
5	96.8 ± 0.1	96.9 ± 0.1	96.7 ± 0.1	96.9 ± 0.0	97.0 ± 0.1
6	96.9 ± 0.1	96.9 ± 0.1	96.9 ± 0.1	97.6 ± 0.0	96.9 ± 0.0

Table 3. Comparison of the accuracy of our method for different given intermediate domains (including source and target domains) on the **Color-Shift MNIST** dataset, as well as the 95% confidence interval of the mean across 5 runs.

# Given Domains	# Inter-domain counts in GDO				
	0	1	2	3	4
2	86.2 ± 0.1	96.5 ± 0.0	87.2 ± 3.6	86.6 ± 0.0	86.6 ± 0.1
3	98.1 ± 0.0	98.2 ± 0.0	98.2 ± 0.0	98.3 ± 0.0	98.3 ± 0.0
4	98.3 ± 0.0	98.3 ± 0.0	98.3 ± 0.0	98.3 ± 0.0	98.3 ± 0.0
5	98.3 ± 0.0	98.3 ± 0.0	98.3 ± 0.0	98.2 ± 0.0	98.3 ± 0.0
6	98.3 ± 0.0	98.3 ± 0.0	98.3 ± 0.0	98.2 ± 0.0	98.2 ± 0.0

Table 4. Comparison of the accuracy of our method for different given intermediate domains (including source and target domains) on the **Portraits** dataset, as well as the 95% confidence interval of the mean across 5 runs.

# Given Domains	# Inter-domain counts in GDO				
	0	1	2	3	4
2	83.7 ± 0.3	84.4 ± 0.8	85.1 ± 0.6	85.1 ± 0.8	85.1 ± 0.5
3	84.1 ± 0.3	84.6 ± 0.2	84.8 ± 0.5	84.7 ± 0.1	84.7 ± 0.2
4	83.8 ± 0.7	84.0 ± 0.1	84.0 ± 0.2	83.8 ± 0.3	83.9 ± 0.1
5	84.8 ± 0.4	84.8 ± 0.4	84.8 ± 0.4	84.8 ± 0.2	84.9 ± 0.4
6	85.3 ± 0.9	86.1 ± 0.4	85.8 ± 1.0	85.6 ± 1.8	85.4 ± 0.9

datasets. The results validate that our GDO better handles continuous distribution shifts compared to static domain alignment approaches like DANN or single-step gradual methods.

Table 5. Comparison of the accuracy of our method for different given intermediate domains (including source and target domains) on the **Cover Type** dataset, as well as the 95% confidence interval of the mean across 5 runs.

# Given Domains	# Inter-domain counts in GDO				
	0	1	2	3	4
2	69.7 ± 0.0	70.0 ± 0.0	70.5 ± 0.1	71.2 ± 0.0	71.8 ± 0.1
3	70.1 ± 0.0	72.3 ± 0.0	73.9 ± 0.0	74.3 ± 0.0	74.4 ± 0.1
4	71.5 ± 0.0	73.8 ± 0.0	74.2 ± 0.0	74.0 ± 0.0	74.2 ± 0.0
5	72.5 ± 0.1	74.2 ± 0.0	74.1 ± 0.0	74.2 ± 0.1	73.9 ± 0.0
6	73.1 ± 0.0	74.1 ± 0.0	73.4 ± 0.0	73.9 ± 0.0	73.4 ± 0.0

We present a comparative analysis of our proposed SWAT method across multiple datasets, namely Rotated MNIST, Color-Shift MNIST, Portraits, and Cover Type, as detailed in Tables 2 to 5. Each experiment was conducted multiple times, and the results are reported as mean values accompanied by their respective variance intervals. The leftmost column of each table displays the performance achieved using adversarial training alone, corresponding to the baseline approach without the incorporation of flow matching.

In Tables 2 to 5, the column labeled “# Given Domains” denotes the total number of domains involved in each experiment, including both source and target domains. The columns titled “Inter-domain counts in SWAT” represent the number of inter-domain steps performed between the specified domains within the dataset. The total number of training steps is given by the expression: $(\# \text{Given Domains} - 1) \times (\# \text{Inter-domain counts in SWAT} + 1) + 1$, which accounts for the self-training procedure involving both the GAN, the encoder f , and the classifier g . For example, when four domains and three intermediate steps are considered, the total number of training steps is calculated as $(4 - 1) \times (3 + 1) + 1 = 13$ small steps.

The experimental results demonstrate the effectiveness of the SWAT method across the datasets under consideration—Rotated MNIST, Color-Shift MNIST, Portraits, and

Cover Type. For each dataset, we varied the number of given domains and the number of inter-domain steps in the SWAT procedure. The performance of the model was evaluated as the number of inter-domain steps increased, providing a detailed analysis of the influence of these factors on the overall effectiveness of the domain adaptation process. In addition, small standard deviations ($\leq 1.2\%$) confirm method reliability.

6.3. Ablation Study

In order to verify the influence of the intermediate domain on the experimental results, we conducted experiments on four datasets without GDO, with 2 domains (i.e., only the source domain and the target domain) to 7 domains (i.e., including 5 intermediate domains). The results are shown in the figure 4. When the intermediate domain is included, the accuracy is greatly improved in most experimental cases compared with the case without the intermediate domain, and the standard deviation is also reduced. This shows that progressive domain adaptation has a great influence on improving domain generalization.

7. Conclusion

In this paper, we introduced Gradual Domain Osmosis (GDO), a novel method for Gradual Domain Adaptation (GDA) that effectively addresses the challenges of smooth knowledge migration across domains. By dynamically adjusting the hyperparameter λ , which balances the weight between the source and target domains, GDO allows for a progressive, efficient transfer of knowledge through a self-training framework. This approach mitigates domain bias, ensuring that the model generalizes well in a progressively adapted intermediate domain. Our experimental evaluations on multiple datasets, demonstrate that GDO outperforms existing state-of-the-art methods in both accuracy and robustness.

Impact Statement

This paper presents work whose goal is to advance the field of Machine Learning. There are many potential societal consequences of our work, none which we feel must be specifically highlighted here.

References

Abnar, S., Berg, R. v. d., Ghiasi, G., Dehghani, M., Kalchbrenner, N., and Sedghi, H. Gradual domain adaptation in the wild: When intermediate distributions are absent. *arXiv preprint arXiv:2106.06080*, 2021.

Blackard, J. Covertype. UCI Machine Learning Repository, 1998. DOI: <https://doi.org/10.24432/C50K5N>.

Bui, M.-H., Tran, T., Tran, A., and Phung, D. Exploiting domain-specific features to enhance domain generalization. *Advances in Neural Information Processing Systems*, 34:21189–21201, 2021.

Chen, H.-Y. and Chao, W.-L. Gradual domain adaptation without indexed intermediate domains. *Advances in neural information processing systems*, 34:8201–8214, 2021.

Chen, Y., Song, S., Li, S., and Wu, C. A graph embedding framework for maximum mean discrepancy-based domain adaptation algorithms. *IEEE Transactions on Image Processing*, 29:199–213, 2020. doi: 10.1109/TIP.2019.2928630.

Damodaran, B. B., Kellenberger, B., Flamary, R., Tuia, D., and Courty, N. Deepjdot: Deep joint distribution optimal transport for unsupervised domain adaptation. In *Proceedings of the European conference on computer vision (ECCV)*, pp. 447–463, 2018.

Deng, L. The mnist database of handwritten digit images for machine learning research. *IEEE Signal Processing Magazine*, 29(6):141–142, 2012.

Dou, Q., Coelho de Castro, D., Kamnitsas, K., and Glocker, B. Domain generalization via model-agnostic learning of semantic features. *Advances in neural information processing systems*, 32, 2019.

Farahani, A., Voghoei, S., Rasheed, K., and Arabnia, H. R. A brief review of domain adaptation. *Advances in data science and information engineering: proceedings from ICDA 2020 and IKE 2020*, pp. 877–894, 2021.

Farshchian, A., Gallego, J. A., Cohen, J. P., Bengio, Y., Miller, L. E., and Solla, S. A. Adversarial domain adaptation for stable brain-machine interfaces. *arXiv preprint arXiv:1810.00045*, 2018.

Ganin, Y. and Lempitsky, V. Unsupervised domain adaptation by backpropagation. In *International conference on machine learning*, pp. 1180–1189. PMLR, 2015a.

Ganin, Y. and Lempitsky, V. Unsupervised domain adaptation by backpropagation. In *International conference on machine learning*, pp. 1180–1189. PMLR, 2015b.

Ganin, Y., Ustinova, E., Ajakan, H., Germain, P., Larochelle, H., Laviolette, F., March, M., and Lempitsky, V. Domain-adversarial training of neural networks. *Journal of machine learning research*, 17(59):1–35, 2016.

Ginosar, S., Rakelly, K., Sachs, S., Yin, B., and Efros, A. A. A century of portraits: A visual historical record of american high school yearbooks. In *Proceedings of the IEEE International Conference on Computer Vision Workshops*, pp. 1–7, 2015.

- He, Y., Wang, H., Li, B., and Zhao, H. Gradual domain adaptation: Theory and algorithms. *arXiv preprint arXiv:2310.13852*, 2023.
- Hoffman, J., Tzeng, E., Park, T., Zhu, J.-Y., Isola, P., Saenko, K., Efros, A., and Darrell, T. Cycada: Cycle-consistent adversarial domain adaptation. In *International conference on machine learning*, pp. 1989–1998. Pmlr, 2018.
- Ioffe, S. and Szegedy, C. Batch normalization: Accelerating deep network training by reducing internal covariate shift. *arXiv preprint arXiv:1502.03167*, 2015. URL <https://arxiv.org/abs/1502.03167>.
- Kang, G., Jiang, L., Yang, Y., and Hauptmann, A. G. Contrastive adaptation network for unsupervised domain adaptation. In *Proceedings of the IEEE/CVF Conference on Computer Vision and Pattern Recognition (CVPR)*, June 2019.
- Kingma, D. P. and Ba, J. Adam: A method for stochastic optimization. *arXiv preprint arXiv:1412.6980*, 2014. URL <https://arxiv.org/abs/1412.6980>.
- Kumar, A., Ma, T., and Liang, P. Understanding self-training for gradual domain adaptation. In *International conference on machine learning*, pp. 5468–5479. PMLR, 2020.
- Li, D., Yang, Y., Song, Y.-Z., and Hospedales, T. Learning to generalize: Meta-learning for domain generalization. In *Proceedings of the AAAI conference on artificial intelligence*, volume 32, 2018.
- Li, J., Wu, Y., and Lu, K. Structured domain adaptation. *IEEE Transactions on Circuits and Systems for Video Technology*, 27(8):1700–1713, 2016.
- Liu, X., Yoo, C., Xing, F., Oh, H., El Fakhri, G., Kang, J.-W., Woo, J., et al. Deep unsupervised domain adaptation: A review of recent advances and perspectives. *APSIPA Transactions on Signal and Information Processing*, 11(1), 2022.
- Marsden, R. A., Döbler, M., and Yang, B. Introducing intermediate domains for effective self-training during test-time. In *2024 International Joint Conference on Neural Networks (IJCNN)*, pp. 1–10. IEEE, 2024.
- Muandet, K., Balduzzi, D., and Schölkopf, B. Domain generalization via invariant feature representation. In *International conference on machine learning*, pp. 10–18. PMLR, 2013.
- Ovadia, Y., Fertig, E., Ren, J., Nado, Z., Sculley, D., Nowozin, S., Dillon, J., Lakshminarayanan, B., and Snoek, J. Can you trust your model’s uncertainty? evaluating predictive uncertainty under dataset shift. *Advances in neural information processing systems*, 32, 2019.
- Pan, S. J. and Yang, Q. A survey on transfer learning. *IEEE Transactions on knowledge and data engineering*, 22(10): 1345–1359, 2009.
- Sagawa, S. and Hino, H. Gradual domain adaptation via normalizing flows. *arXiv preprint arXiv:2206.11492*, 2022.
- Sagawa, S. and Hino, H. Gradual domain adaptation via normalizing flows. *Neural Computation*, pp. 1–47, 2025.
- Shi, L. and Liu, W. Adversarial self-training improves robustness and generalization for gradual domain adaptation. *Advances in Neural Information Processing Systems*, 36, 2024.
- Srivastava, N., Hinton, G., Krizhevsky, A., Sutskever, I., and Salakhutdinov, R. Dropout: A simple way to prevent neural networks from overfitting. *Journal of Machine Learning Research*, 15(56):1929–1958, 2014. URL <https://www.jmlr.org/papers/v15/srivastava14a.html>.
- Sun, B. and Saenko, K. Deep coral: Correlation alignment for deep domain adaptation. In *Computer Vision—ECCV 2016 Workshops: Amsterdam, The Netherlands, October 8–10 and 15–16, 2016, Proceedings, Part III 14*, pp. 443–450. Springer, 2016.
- Tang, H. and Jia, K. Discriminative adversarial domain adaptation. In *Proceedings of the AAAI conference on artificial intelligence*, volume 34, pp. 5940–5947, 2020.
- Tzeng, E., Hoffman, J., Saenko, K., and Darrell, T. Adversarial discriminative domain adaptation. In *Proceedings of the IEEE Conference on Computer Vision and Pattern Recognition (CVPR)*, July 2017.
- Volpi, R., Morerio, P., Savarese, S., and Murino, V. Adversarial feature augmentation for unsupervised domain adaptation. In *Proceedings of the IEEE Conference on Computer Vision and Pattern Recognition (CVPR)*, June 2018.
- Wang, H., Li, B., and Zhao, H. Understanding gradual domain adaptation: Improved analysis, optimal path and beyond. In *International Conference on Machine Learning*, pp. 22784–22801. PMLR, 2022a.
- Wang, Y., Qi, L., Shi, Y., and Gao, Y. Feature-based style randomization for domain generalization. *IEEE Transactions on Circuits and Systems for Video Technology*, 32(8):5495–5509, 2022b.
- Xie, Q., Luong, M.-T., Hovy, E., and Le, Q. V. Self-training with noisy student improves imagenet classification. In *Proceedings of the IEEE/CVF conference on computer vision and pattern recognition*, pp. 10687–10698, 2020.

- Yan, H., Ding, Y., Li, P., Wang, Q., Xu, Y., and Zuo, W. Mind the class weight bias: Weighted maximum mean discrepancy for unsupervised domain adaptation. In *Proceedings of the IEEE Conference on Computer Vision and Pattern Recognition (CVPR)*, July 2017.
- Yang, J., Zou, H., Zhou, Y., Zeng, Z., and Xie, L. Mind the discriminability: Asymmetric adversarial domain adaptation. In *Computer Vision—ECCV 2020: 16th European Conference, Glasgow, UK, August 23–28, 2020, Proceedings, Part XXIV 16*, pp. 589–606. Springer, 2020.
- Zhang, W., Ouyang, W., Li, W., and Xu, D. Collaborative and adversarial network for unsupervised domain adaptation. In *Proceedings of the IEEE Conference on Computer Vision and Pattern Recognition (CVPR)*, June 2018.
- Zhang, Y., Deng, B., Jia, K., and Zhang, L. Gradual domain adaptation via self-training of auxiliary models. *arXiv preprint arXiv:2106.09890*, 2021.
- Zhao, H., Des Combes, R. T., Zhang, K., and Gordon, G. On learning invariant representations for domain adaptation. In *International conference on machine learning*, pp. 7523–7532. PMLR, 2019.
- Zhao, S., Yue, X., Zhang, S., Li, B., Zhao, H., Wu, B., Krishna, R., Gonzalez, J. E., Sangiovanni-Vincentelli, A. L., Seshia, S. A., et al. A review of single-source deep unsupervised visual domain adaptation. *IEEE Transactions on Neural Networks and Learning Systems*, 33(2):473–493, 2020.
- Zhuang, Z., Zhang, Y., and Wei, Y. Gradual domain adaptation via gradient flow. In *The Twelfth International Conference on Learning Representations*, 2024.